# Three-Body Correlations in the Metallic Glass $Ni_{81}B_{19}$ Probed by X-Ray-Absorption Near-Edge-Structure Spectroscopy

Peter Kizler

*Hamburger Synchrotronstrahlungslabor (HASYLAB) at Deutsches Elektronen-Synchrotron (DESY), Notkestrasse 85, W-2000 Hamburg 52, Germany*

(Received 19 August 1991)

Practical information on higher-order correlations in a metallic glass, $Ni_{81}B_{19}$, is derived from x-ray-absorption near-edge-structure (XANES) data. For the structure of amorphous $Ni_{81}B_{19}$, a statistical evaluation of XANES calculations revealed that a minority of Ni-Ni-B triangles with peculiar shapes and sizes is to a significnat degree responsible for the appearance of the experimental XANES features. The two most relevant types of triangles have one Ni-Ni and one Ni-B distance of about 0.25 nm and 0.20 nm each, identical with the average atomic distances of diffraction data. The second Ni-B distance was found to be sharply defined as $0.195 \pm 0.005$ or $0.275 \pm 0.015$ nm in either type.

PACS numbers: 61.10.Lx, 61.42.+h, 71.25.Mg

Techniques for determining atomic arrangements like diffraction or extended x-ray-absorption fine-structure (EXAFS) spectroscopy usually give only the pair-correlation functions of the system. They describe the deviation of the atomic density of $j$ atoms around $i$ atoms from the average density of the material.

In the case of crystalline materials with their full lattice structure, all higher-order correlations (like bond angles) are implied and do not provide any additional information about the structure. In the case of disordered solids or liquids the terms of pair correlations and higher-order correlations, however, are partly decoupled, and knowledge of the latter promises valuable additional information about the structure of the material [1,2]. Yet pair and higher-order correlations can never be completely independent, because the necessity to fill a given space densely with atoms restricts the choices of possible atomic arrangements. Because of the nature of the disordered (or distorted) structure, such higher-order correlations can probably not be attributed to one single structural element like a unit cell or a coordination polyhedron. Instead, a statistical description of the abundance of structural features has to be taken into account.

A promising approach to study many-body-correlations centers on the interpretation of the near-edge structure region of the x-ray-absorption spectrum (XANES). Within roughly 50 eV beyond the absorption edge, the electrons emitted by the x-ray-absorbing atom undergo multiple scattering events and thereby interact with many other atoms. Durham, Pendry and Hodges [3,4] and Vvedensky, Saldin, and Pendry [5] provided powerful algorithms to numerically simulate experimental XANES data. Such calculations yield theoretical XANES spectra based on geometrical trial structures. Depending on the agreement between simulated and experimental data, the merit of a trial structure can be evaluated. Test calculations [3,6] have already demonstrated the sensible connection between simulated XANES results and bond angles in the trial structure.

XANES spectra of the Fe and Ni edges in amorphous $Fe_{80}B_{20}$ and $Ni_{81}B_{19}$ have previously been simulated [7] in good agreement with experimental data recorded at the ROEMO II station of HASYLAB at DESY. The structures of the Fe and Ni alloys were tentatively treated as identical, neglecting the small differences between the atomic distances [8,9]. This previous study made use of five different structural models proposed for the alloys. All agreed well with other experimental data [8,9] under the aspect of their partial pair-correlation functions, and were very similar under the aspect of angular correlation functions and statistical distribution of coordination numbers [10]. A random choice of 40 central metal atoms out of each model (hereafter to be called "core" atoms), together with their cluster of surrounding atoms within a sphere of 0.55 nm radius, had served as input for the XANES simulations. The average of the 40 single simulations formed the XANES result (Fig. 1) for each model. Multiple scattering had been included in the calculations. While the peaks around 28 and 58 eV were reproduced similarly well for all models, the essential difference among the results was how well the hump around 40 eV was reproduced by the calculations. The model of

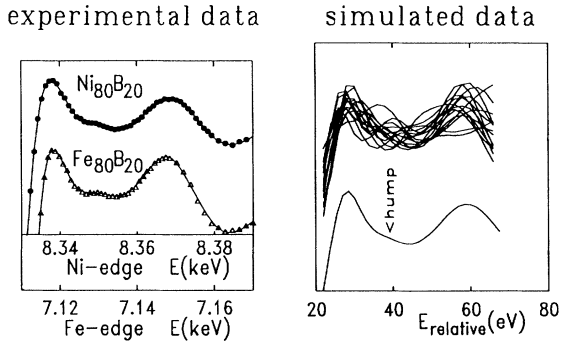


FIG. 1. Left: experimental XANES data for the metal edges in amorphous $Ni_{80}B_{20}$ and $Fe_{80}B_{20}$ alloys. The data were recorded [7] at the ROEMO II station of HASYLAB, DESY. Right: random selection out of 322 individual XANES calculation results (upper curves) and averaged result from all 322 curves for the model of Dubois, Gaskell, and Le Caër (lowest curve).

Dubois, Gaskell, and Le Caër [11] agreed best with the simulated and the experimental data, but even for this model the 40-eV hump did not reproduce very satisfactorily.

More elaborate calculations, removing either the multiple scattering part altogether (see Ref. [5]), or the boron atoms within the first coordination sphere, made evident that the 40-eV peak arises from contributions of multiple scattering (i.e., any structural feature consisting of more than two atoms) and of boron atoms rather than of metal atoms. The 28- and 50-eV peaks, simply reflecting the atomic distances, were largely unaffected by the computational manipulations. Evidently, the XANES feature around 40 eV hides some additional information about the structure of the two metallic glasses.

In order to elucidate the nature of the peculiar XANES feature around 40 eV, the calculations were extended to a larger body of 322 nickel core atoms taken from the total number of 1821 atoms of the model of Dubois, Gaskell, and Le Caër, along with their surrounding clusters of neighboring atoms. The core atoms were chosen such that the outward boundaries of the ensuing large clusters lay well within the perimeter of the model. The same procedure as in Ref. [7] was followed, utilizing the identical scattering phase shifts and the model of Dubois, Gaskell, and Le Caër only.

The 322 individual XANES results were visually sorted into different categories of curve shapes. From the multitude of individual curve shapes, four major categories could be discerned, of which two were most pronounced.

The first were curves with a clear three-peak outline (44 in total, with a very prominent peak at an energy of 40 eV, hereafter termed "*P* type") and the second were curves with a distinct minimum at 40 eV (102 in total, hereafter termed "*Q* type"). The respective Ni core atoms giving rise to these particular curve shapes will be termed "*P* atoms" and "*Q* atoms" in the following. The overall *P*-type and *Q*-type curves averaged from the total number of curves for each type are plotted in Fig. 2. As well as the *P*- and *Q*-type curves, there were another 166 curves with a poorly defined structure with neither a pronounced peak nor a clear minimum, and 10 curves with irregular shapes in disagreement with all the other categories. The total sum curve of all XANES results (Fig. 1, bottom curve) was practically identical with the one from the earlier calculations. Comparing the *P*-type (upper) curve in Fig. 2 and the total sum (bottom) curve of Fig. 1, it appears that a larger fraction of *P* atoms (i.e., *P* curves) would further improve the agreement between theory and experiment.

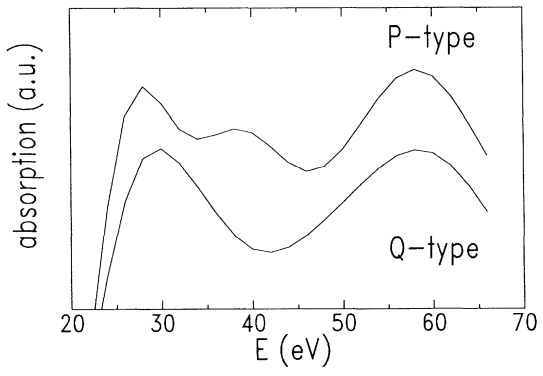


FIG. 2. Averaged simulated XANES curves of the *P* and *Q* type, obtained from the structural model of Dubois, Gaskell, and Le Gaër.

Again, the XANES calculations for the *P*-type and *Q*-type core atoms were manipulated and performed with the same additional restrictions as before, i.e., removing either the multiple-scattering paths, or the boron atoms within the first coordination sphere. Figure 3 shows the results for the *P*-type atoms together with the unmanipulated original result from Fig. 2. Evidently both manipulations, as they cause the 40-eV peak to decrease, reveal an intimate relation between this peak and both the boron atoms and electron multiple scattering. For the *Q*-type atoms, the curve shapes did not respond to the same manipulative calculations and no meaningful change in curve shape could be detected.

In order to check if variations in the number densities could account for the two curve types, the radial Ni-Ni and Ni-B number densities were calculated from the coordinates of the model of Dubois, Gaskell, and Le Caër with a simple integration procedure and a step width of 0.004 nm. The calculations were performed for the whole model and for *P* and *Q* atoms separately. The very small differences found cannot be made responsible for the large differences between the *P* and *Q* curves [12].

A probable electron multiple-scattering path is a triangular path back to the x-ray absorbing atom. There-

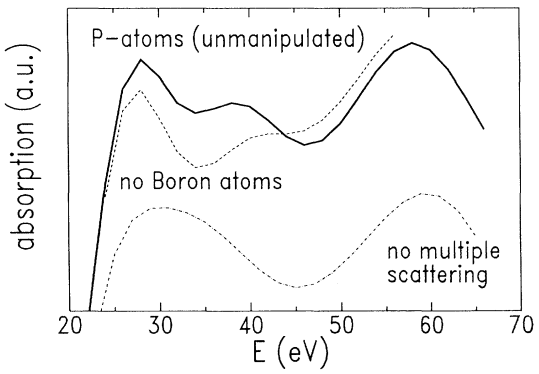


FIG. 3. Simulated XANES curves for the *P*-type atoms with certain restrictions. Top curve (bold): calculation as in Fig. 2, multiple scattering and B atoms included. Middle curve (dashed): B atoms removed from the first coordination shell. Bottom curve (dash-dotted): multiple scattering "switched off" (i.e., only single scattering), B atoms included.

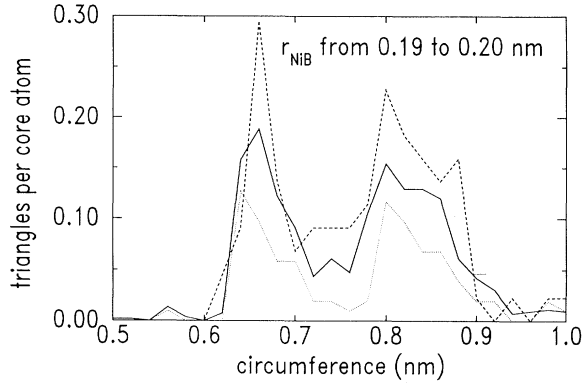


FIG. 4. Average number of triangles per Ni core atom in the model of Dubois, Gaskell, and Le Caër with $r_{\mathrm{Ni(core)\text{-}B}}$ below 0.2 nm and $r_{\mathrm{Ni(core)\text{-}Ni}}$ below 0.32 nm. Solid curve: whole model; dashed curve: $P$-type core atoms; dotted curve: $Q$-type core atoms.

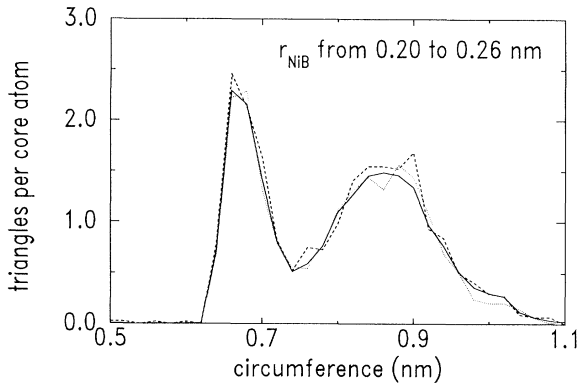


FIG. 5. Average number of triangles per Ni core atom in the model of Dubois, Gaskell, and Le Caër with $r_{\mathrm{Ni(core)\text{-}B}}$ between 0.20 and 0.26 nm and $r_{\mathrm{Ni(core)\text{-}Ni}}$ below 0.32 nm. Solid curve: whole model; dashed curve: $P$-type core atoms; dotted curve: $Q$-type core atoms.

fore it seemed reasonable to use the circumference of triangles with a Ni core atom as an apex as a first probe into the problem. Highly significant differences between the overall model and the $P$- and $Q$-type core atoms were obtained from a statistical examination of triangles consisting of a Ni core atom and a neighboring Ni and B atom. As it turned out, significant results could only be obtained when the Ni(core)-B distance was precisely defined. Conversely, the Ni(core)-Ni distance could be fixed within a large tolerance and simply had to range within the first coordination sphere, i.e., below 0.32 nm. For each metal core atom to be examined, Ni and B neighboring atoms were selected within a range of distances to form Ni-Ni-B triangles with the core atom. The circumference of each triangle was calculated and these were sorted by value with a step width of 0.02 nm. Finally, the total number of collected triangles was divided by the number of examined core atoms. Thus the abscissa of the following diagrams expresses the average number of triangles per Ni core atom met in a given interval of circumferences.

Figures 4–6 show the results for different classes of triangles. The range of Ni(core)-B radii is $0.19 < r < 0.20$ nm for Fig. 4, $0.20 < r < 0.26$ nm for Fig. 5, and $0.26 < r < 0.29$ nm for Fig. 6. The Ni(core)-Ni distance was confined within $r < 0.32$ nm in all three cases. Whereas the results for the $P$- and $Q$-type atoms and the result for the overall model do not differ for the intermediate Ni(core)-B distance (Fig. 5), there appears a highly significant difference between the atom types and the overall model for the short and the long Ni(core)-Bi distance (Figs. 4 and 6).

For all classes of triangles, the first peak around a circumference of approximately 0.7 nm corresponds to triangles with all atoms adjacent. For the circumferences between 0.8 and 1.0 nm, the sides of the triangles opposite to the core atom have lengths between 0.4 and 0.5 nm. This already ranges into the second maximum of the partial pair-correlation function $G_{\mathrm{NiB}}$ (see Refs. [8] and [9]) and reaches beyond the immediate short-range order.

Therefore, even larger triangles were investigated (Fig. 7). A consistent picture emerged when the Ni(core)-Ni distance fell between 0.40 and 0.48 nm (approximately the range of the opposite triangle edge, as above) with the Ni(core)-B distances ranging from 0.26 to 0.29 nm (i.e., $\approx$ the "long" Ni-B distance; compare Fig. 6). Always relying on the validity of the structural model, the persistence of the significant differences between $P$- and $Q$-type Ni core atoms and the overall model, even for the large triangles with a circumference of 1.3 nm, demonstrates the existence of three-body correlations even between the Ni core atoms and the second metal-metal coordination shell. The corresponding partial pair-correlation functions $G_{\mathrm{NiNi}}$ and $G_{\mathrm{FeFe}}$ were derived earlier from neutron-diffraction experiments [8,9].

Statistical evaluations like the ones above were also performed for triangles consisting of Ni atoms only, but it was not possible to find any significant difference between the $P$ and $Q$ atoms and the whole model's core atoms with respect to the distribution of metal triangles.

The three-body correlations as revealed by the statistics of triangles in the structure should now be a challenge to the theory of metallic glasses to study the role of these peculiar structural elements. While the smallest triangles with the Ni(core)-B distance below 0.20 nm and a circumference of $\approx 0.66$ nm (Fig. 4) are easily conceived as just Ni and B atoms at the closest possible distance, a Ni-B distance of $0.275 \pm 0.015$ nm (Fig. 6) is more difficult to understand. The value is much larger than the average Ni-B distance [9] and still larger than, for instance, the distance between the B atom at the center of a trigonal prism and a Ni cusp atom capping a square face of that prism [13].

Despite their obvious responsibility for the particular XANES features of $Ni_{81}B_{19}$, the mentioned triangles are still a minority in the neighborhood of the $P$ atoms, which

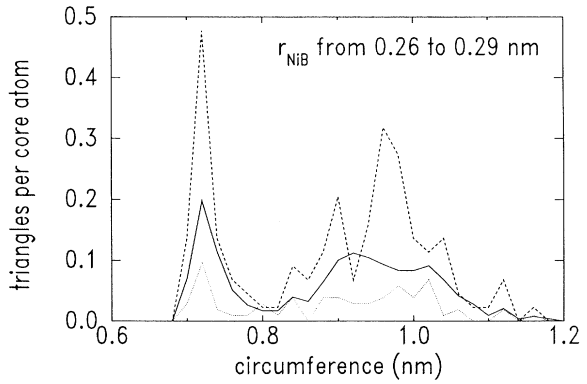


FIG. 6. Average number of triangles per Ni core atom in the model of Dubois, Gaskell, and Le Caër with $r_{Ni(core)-B}$ between 0.26 and 0.29 nm and $r_{Ni(core)-Ni}$ below 0.32 nm. Solid curve: whole model; dashed curve: *P*-type core atoms; dotted curve: *Q*-type core atoms.

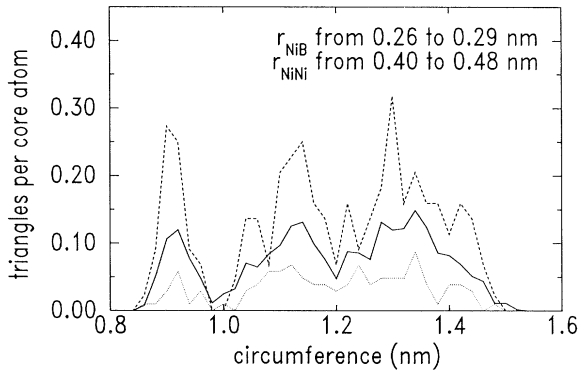


FIG. 7. Average number of triangles per Ni core atom in the model of Dubois, Gaskell, and Le Caër with $r_{Ni(core)-B}$ between 0.26 and 0.29 nm and $r_{Ni(core)-Ni}$ between 0.40 and 0.48 nm. Solid curve: whole model; dashed curve: *P*-type core atoms; dotted curve: *Q*-type core atoms.

themselves are a minority in the whole model. Therefore, the triangles are neither a structure-determining entity nor representative of the structure—they have to be regarded as a significant modifier.

We stress that the above results do not solely rely on the application or correctness of the model of Dubois, Gaskell, and Le Caër. Essentially the same calculations have recently been carried out on the basis of Zweck's model [14]. The general trend of the results was confirmed and details from these calculations as well as from the treatment of another metallic glass by the new method will be the subject of a forthcoming paper [12].

The present study demonstrates the power of numerical XANES simulation to sense three-body correlations in a disordered material and to gain a more detailed understanding of experimental XANES data. In the case of the metallic glasses $Ni_{81}B_{19}$ and $Fe_{80}B_{20}$, the reason for the successful XANES simulation from the model of Dubois, Gaskell, and La Caër was found to rest upon the metal-metal-boron triangles of several well-defined sizes. The smallest ones consist of three atoms with the closest possible packing distances. Larger ones demonstrate the impact of structural elements which have not yet attracted attention as characteristic "bricks" in the theory of metallic glasses. It must be kept in mind, however, that, surprisingly enough, these triangles do form a minority within the whole structure. Finally, if the model of Dubois, Gaskell, and Le Caër were modified to incorporate a larger number of the triangles in question (i.e., if the number of *P*-type core atoms would be increased), the agreement between experiment and theoretical calculation could certainly be further improved.

Critical reading and many valuable comments by U. Löchner, Technical University of Darmstadt, while writing this paper are gratefully acknowledged.

[1] P. A. Egelstaff, *An Introduction to the Liquid State* (Academic, London, 1967).

[2] *Proceedings of the Workshop on Investigations of Higher Order Correlation Functions "Beyond Radial Distribution," Grenoble, France, 15–16 July 1985,* edited by J. B. Suck, D. Quitman, and B. Maier [J. Phys. (Paris), Colloq. **46**, C9 (1985)].

[3] P. J. Durham, J. B. Pendry, and C. H. Hodges, Solid State Commun. **38**, 159 (1981).

[4] P. J. Durham, J. B. Pendry, and C. H. Hodges, Comput. Phys. Commun. **25**, 193 (1982).

[5] D. D. Vvedensky, D. K. Saldin, and J. B. Pendry, Comput. Phys. Commun. **40**, 421 (1986).

[6] P. Kizler and S. Steeb, in *Proceedings of the Fifth XAFS Conference, Seattle, Washington, 21–26 August 1988,* edited by J. M. de León *et al.* [Physica (Amsterdam) **158B**, 392 (1989)].

[7] P. Kizler, P. Lamparter, and S. Steeb, Z. Naturforsch. **44a**, 189 (1989), and references therein; P. Kizler, Ph.D. thesis, University of Stuttgart, Germany, 1988 (unpublished).

[8] E. Nold, P. Lamparter, H. Olbrich, G. Rainer-Harbach, and S. Steeb, Z. Naturforsch. **36a**, 1032 (1981).

[9] P. Lamparter, W. Sperl, S. Steeb, and J. Blétry, Z. Naturforsch. **37a**, 1223 (1982).

[10] P. Kizler, P. Lamparter, and S. Steeb, Z. Naturforsch. **43a**, 1047 (1988).

[11] J. M. Dubois, P. H. Gaskell, and G. Le Caër, Proc. R. Soc. London A **402**, 323 (1985).

[12] P. Kizler (to be published).

[13] See, e.g., Fig. 10 related discussion in Ref. [9].

[14] U. Krey, H. Ostermeier, and J. Zweck, Phys. Status Solidi (b) **144**, 203 (1987); J. Zweck, Ph.D. thesis, University of Regensburg, Germany, 1987 (unpublished).